SYNTHESIS, CHARACTERIZATION AND PHOTOCATALYTIC ACTIVITY OF Mn-Fe CODOPED CdS NANOCOMPOSITE ON THE DEGRADATION OF METHYLENE BLUE UNDER VISIBLE LIGHT IRRADIATION

M Sc GRADUATE PROJECT

MISGANA TOLESA BAYISA

AUGUST 2017

HARAMAYA UNIVERSITY, HARAMAYA

Synthesis, Characterization and Photocatalytic Activity of Mn-Fe Codoped CdS Nanocomposite on the Degradation of Methylene Blue under Visible Light Irradiation

A Graduate Project Submitted to the College of Natural and Computational Sciences, Department of Chemistry,
HARAMAYA UNIVERSITY

In Partial Fulfillment of the Requirements for the Degree of
MASTER OF SCIENCE IN CHEMISTRY (INORGANIC CHEMISTRY)

Misgana Tolesa Bayisa

December 2017

Haramaya University, Haramaya

HARAMAYA UNIVERSITY

POSTGRADUATE PROGRAM DIRECTORATE

I hereby certify that we have read and evaluated this Thesis titled "***Synthesis, Characterization and Photocatalytic Activity of Mn-Fe Codoped CdS Nanocomposite on the Degradation of Methylene Blue under Visible Irradiation***"prepared under my guidance by Misgana Tolesa. We recommended that it be submitted as fulfilling the project requirement.

Tesfahun Kebede (PhD)	_____	_____
Name of Major Advisor	Signature	Date

As members of the Board of examiners of the M.Sc. project open Defense Examination, I certify that I have read, evaluated the project prepared by Misgana Tolesa and examined the candidate. I recommend that the project be accepted as fulfilling the project requirement for the Degree of Master of Science in Chemistry (Inorganic Chemistry*)*.

_____	_____	_____
Chairperson	Signature	Date
_____	_____	_____
Internal Examiner	Signature	Date
_____	_____	_____
External Examiner	Signature	Date

Final approval and acceptance of the thesis is contingent upon the submission of its final copy to the Council Graduate Studies (CGS) through the candidate's department or school graduate committee (DGC or SGC).

DEDICATION

This manuscript is dedicated to my beloved families for nursing me with affection and love and for their dedicated partnership in the success of my life

STATEMENT OF THE AUTHOR

By my signature below, I declare and affirm that this project is my own work. I have followed all ethical and technical principles of scholarship in the preparation, data collection, data analysis and completion of this project. Any scholarly matter that is included in the project has been given recognition through citation.

This project is submitted in partial fulfillment of the requirements for Master Of Science In Chemistry (Inorganic Chemistry) at the Haramaya University. This project deposited in the Haramaya University library and is made available to borrowers under the rules of the library.

I solemnly declare that this project has not been submitted to any other institution for the award of any academic degree, diploma, or certificate.

Brief quotations from this project may be made without special permission provided that accurate and complete acknowledgement of the source is made. Requests for permission for extended quotations from or reproduction of this manuscript in whole or in part may be granted by the Head of the School or Department when in his or her judgment the proposed use of the material is in the interest of scholarship. In all other instances, however, permission must be obtained from the author of the project.

Name: Misgana Tolesa

Place: Haramaya University

Date of Submission:

Signature:

BIOGRAPHICAL SKETCH

The author was born on August 2, 1983 G.C in Homi Kebele, Abay Chommen Woreda, Horo Guduru wollega Zone in Oromia Regional State. He attended his primary education at Homi Elementary School and secondary education at Shambu Comprehensive Senior Secondary School.After completing preparatory School, He joined Jimma University in 1996 and graduated in june, 1998 with B.ED Degree in Chemistry. He was employed as teacher at Kellam Wollega School, in September 1999. He worked there for four years and then joined School of Graduate studies at Haramaya University, College of Natural and Computational Sciences, Department of Chemistry in 2010 to pursue his M.Sc.

ACKNOWLEDGMENTS

I am deeply thankful to my advisor Dr.Tesfahun Kebede for his invaluable and stimulating interest and unreserved support most generously given to me during the course of my study. I pay respect and express indebtedness to him because of his guidance, consistent supervision as well as suggestions in every phase of the project research work that made it possible to materialize.

My sincere thank also goes to Mr. Fituma Diriba who arranged to me some chemicals and apparatus during the course of this research work. Successful and timely accomplishment of this study would have been difficult without his cooperation.

Last, but not least, I thank the Chemistry Department of Haramaya University for hosting me to pursue my M.Sc. study.

LIST OF ACRONYMS ABBREVATIONS

AOPs	Advanced Oxidation Processes
CB	Conduction Band

Eg	Band Gap Energy
eV	Electron-Volts
GSE	Geological Survey of Ethiopia
MB	Methylene Blue
MO	Methyl Orange
NP	Nanoparticle
TM	Transition Metal
UV-Vis	Ultra Violet visible
VB	Valance Band
XRD	X-ray Diffraction
Pzc	Point of Zero charge

TABLE OF CONTENTS

LIST OF TABLES

Table

pages

LIST OF FIGURES

F i g u r e s

page

LIST OF TABLES IN APPENDIX

Appendix Table
Page

LIST OF FIGURES IN APPENDIX

Appendix Figures
pages

Synthesis, Characterization and Photocatalytic Activity of Mn-Fe Codoped CdS Nanocomposite for the Degradation of Methylene Blue under Visible Light Irradiation

ABSTRACT

Undoped and Fe-Mn codoped CdS nanoparticles have been synthesized via precipitation method. The nanostructures of the prepared undoped and Fe-Mn codoped CdS nanoparticles have been confirmed using UV/Vis absorption and X-ray diffraction analysis. The UV/Visible spectroscopy studies showed that the absorption peak for Fe-Mn codopedCdS has undergone a red shift toward visible wavelengths compared with the CdS nanoparticles. Photocatalytic efficiency of Fe-Mn codopedCdS nanoparticle was investigated for the degradation of MB under visible light irradiation. The results showed that Fe-Mn codopedCdS nanoparticles have exhibited greater photocatalytic activity when compared with the undoped CdS nanoparticle under visible light irradiation. According to these results, application of Fe-Mn on the surface of CdS nanoparticles has caused enhanced photocatalytic activity owing to its greater degradation efficiency. The reduction in absorbance of dye suggests that the dye

molecules were mineralized along with color removal. According to these result, oxidation of the MB consumes photo-generated holes and/or • OH radicals efficiently, blocking the electron-hole recombination and thus, increasing the total efficiency. Influences of some operational parameters such as: amount of photocatalyst, pH of solution, and MB initial concentration on the photodegradation reaction rate were investigated. The optimum values of pH and catalyst dose were found to be 4 and 150 mg/L, respectively for MB intial concentration of10 mg/L.

Keywords:*CdS,doping,dye,nanoparticle,Photocatalyst,VisibleLight,andXRD*

1. INTRODUCTION

Large quantities of colored dye effluents discharged from manufacturing and processing in the textile industry, create severe environmental pollution problems due to their negative impact on photosynthetic activity (Zainal *et al*., 2005). Additionally, variety of a wide range of organic pollutants especially pesticides and dyes are introduced into the water system from various sources such as industrial effluents, agricultural runoff and chemical spills (Cohen *et al*.,1986 ; Muszka et al.,1994). Their toxicity, stability to natural decomposition and persistence in the environment has been the cause of much concern to the societies and regulation authorities around the world. Recently, due to the rapid development of the textile industry more and more new types of dye have been produced, such as methylene blue (Tang *et al*., 2003 ; Jian-xiao *et al*., 2011).

Methylene blue (MB) is one of the thiazine dyes which is hard to be degraded, and it usually acts as the model object of photocatalytic degradation with TiO_2 (Tang *et al*., 2003) and has harmful effects on living things. For example, during inhalation, it can give rise to short periods of rapid or difficult breathing, while ingestion through the mouth produces a burning sensation and may cause nausea, vomiting, diarrhea and gastritis (Abdullah *et al*., 1990). Therefore, decolorisation and detoxicity of these dyes in effluents have received increasing attention.

Conventional methods used to treat dye effluents are classified as physical, biological or chemical methods each having its own drawbacks (Robinson *et al*., 2001). Physical methods such as chemical or electro-flocculation, reverse osmosis and adsorption are not destructive and mainly create pollutant concentrates. Activated sludge process does not work efficiently due to high solubility of synthetic dyes and their resistance to aerobic degradation. Furthermore, dyes, although not directly toxic, may generate carcinogenic compounds such as aromatic amines from azo dyes during their anaerobic treatment (Ledakowicz *et al.,* 1999). Thus, new treatment methods are necessary for the removal of persistent dye chemicals or converting them into harmless compounds in water. Recent studies have shown that heterogeneous semiconductor

(TiO_2, CdS and ZnO) photocatalysis can be an alternative to conventional methods for the removal of dye pollutants from water (Carraway *et al*., 1994; Kyung et al., 2005).

In particular cadmium sulfide is an important semiconducting material that has attracted much interest owing to their unique electronic and optical properties, and their potential applications in solar energy conversion, photoconducting cells, non-linear optics and heterogeneous photocatalysis (Verma *et al*., 2010 ; Murugadoss, 2012).

Transition metal sulphides have unique catalytic functions as a result of the rapid generation of electron-hole pairs by photo-excitation and the highly negative reduction potentials of excited electrons. Moreover, incorporation of transition metal ion dopants in these semiconductor nanoparticles can influence their photocatalytic performance (Stroyuk *et al.*, 2007). The effect of doping on the activity of photocatalyst is governed by several factors, e.g. the type and concentration of dopants, preparation method, the structure and the initial concentration of the pollutants and chemical properties of the catalyst. The increase in charge separation efficiency will enhance the formation of both free hydroxyl radicals and active oxygen species (Kato *et al.,* 2005).

Cadmium sulfide (CdS) with a direct band gap of 2.42 eV at room temperature (RT) is a useful candidate for solar cells, green lasers, photoconductors, light emitting diodes, and thin film transistors (Lee et al., 2007). Transition metal (Mn, Fe, Co, etc.,) doped CdS has drawn considerable attention as it offers a great opportunity to integrate electrical, optical and magnetic properties into a single material, which makes it an ideal candidate for nonvolatile memory, magneto-optical and future spintronic devices (Kulkarnie *et al*., 2006).

The extended life time of charge carriers as observed in Mn doped CdS, for example, could be advantageous to improve the performance of solar energy conversion systems. When doping with Mn, for example, the photoinduced electrons in the conduction band of CdS are transferred to the Mn transtion state, which temporarily traps the electrons and prevents recombination with holes or oxidized electrolyte species (Liu *et al.,* 2012). Mn^{2+} doped CdS NPs are interesting because of

the fact that Mn^{2+} ions provide good traps for the excited electrons, which give rise to their potential use in nonlinear optics, electronic and optoelectronic devices (Hullavarad *et al*., 2008; Nag *et al*., 2010).

Large numbers of studies have been reported on photocatalytic activity for the purpose of improving the photocatalytic efficiency of semiconductor catalysts. Though various modification techniques are reported in doping semiconductors to increase photocatalytic activity, little work has been done to date on transition metal doping to CdS semiconductor. More specifically, no work has been reported so far on the synthesis, characterization and photocatatic activity of Mn and Fe co-doped CdS nanocomposite for the degradation of methylene blue under visible light irradiation. Therefore, this project studies the synthesis, characterization and photocatatic activity of Mn and Fe co-doped CdS nanocomposite for the degradation of methylene blue under visible light irradiation. To optimize the photocatalytic activity, additional parameters such as pH effect, photocatalyst load and dye initial concentration were also investigated.

Objective of the study

General objective

- To Study the photocatalytic degradation efficiency of Mn-Fe codoped cadmium sulfide (CdS) nanocomposite towards degradation of methylene blue under visible light irradiation.

Specific objectives:

The specific objectives of this study were to:

- Synthesize nanosized CdS and Mn-Fe codoped CdS nanocomposite by precipitation method.
- Characterize the as- synthesized Mn-Fe codoped CdS nanocomposite using XRD and UV/Vis analytical techniques.
- Evaluate the photocatalytic degradation efficiency of Mn-Fe codoped CdS nanocomposite towards degradation of Methylene blue.
- Determine the effect of initial dye concentration, pH and amount of photocatalytic loading on photocatalytic activities of the photocatalyst for the degradation of Methylene blue.

2. REVIEW OF LITERATURE

2.1. Principles of Photocatalysis

Photocatalysis is a reaction which uses light to activate a substance which modifies the rate of a chemical reaction without being involved itself. The photocatalyst is a substance which can modify the rate of chemical reaction using light irradiation. Dyes are important class of aquatic pollutants and are becoming a major source of environmental contamination. As the international environmental standards are becoming more stringent, many research studies have been focused on the treatment of colored wastewater. However, because of the complexity and variety of dyestuffs employed in the dyeing process, it has become rather difficult to find a unique treatment procedure that entirely covers the effective elimination of all types of dyes. Particularly, biochemical oxidation suffers from significant limitations since most dyestuffs commercially available have been intentionally designed to resist aerobic microbial degradation and are converted to toxic or carcinogenic compounds. Physical methods such as flocculation, reverse osmosis and adsorption on activated charcoal are non-destructive and merely transfer the pollutants to other media, thus causing secondary pollution (Belver *et al*., 2006).

Photocatalyst particles' band structure is composed of a low energy valence band (VB) filled with electrons and an empty high energy conduction band (CB), which are separated by forbidden band. When exposed to radiation of energy equal or more than the forbidden band gap, VB electrons on the surface may absorb the light energy to transit to the CB. Then the CB gets electrons with reducibility, while the VB produces holes possessing oxidizability. These electrons and holes can move to the surface of the catalyst under suitable light energy, and can react with other substances adsorbed at photocatalyst surface. In addition, they can react with deliquescent oxygen and water while suspended in liquid producing hydroxyl radicals with high chemical activity, which can oxidize the organic pollutants into CO_2, H_2O and N_2, and also attain a purpose of reducing the Chemical Oxygen Demand (COD) of waste water (Lecheng and Dacui, 2001).

The possible mechanism of degradation of organic compound using an irradiated photocatalyst (CdS) is described below.

$$CdS + hv \rightarrow h^+ + e^-$$

H_2O $H^+ + OH^-$

$h^+ + OH^-$ atVB $HO\cdot$

$h^+ + H_2O$ at VB $H^+ + \cdot OH$

$e^- + O_2$ at CB $O_2\cdot^-$

$O_2\cdot^- + H^+$ $HO_2\cdot$

$2HO_2\cdot$ $O_2\cdot + H_2O_2$

$H_2O_2 + O_2\cdot^-$ $\cdot OH + \cdot OH + O_2$

$H_2O_2 + hv$ $2\cdot OH$

Organic $+\cdot OH + O_2$ $CO_2 + H_2O$ + other production

Where: hv- is photon energy required to excite the semiconductor electron from the valence band (VB) to conduction band (CB).

Photons with energies greater than the band-gap energy (Eg) can result in the excitation of valence band (VB) electrons which then promote the possible reactions with organic pollutants. The absorption of photons with energy lower than Eg or longer wavelengths usually causes energy dissipation in the forms of heat. The illumination of the photocatalytic surface with sufficient energy, leads to the formation of a positive hole (h^+) in the valence band and an electron (e-) in the conduction band (CB). The positive hole oxidizes either pollutant directly or water to produce hydroxyl radical ·OH, where as the electron in the conduction band reduces the oxygen adsorbed on the photocatalyst(CdS).

2.2. Photocatalytic Oxidation of Organic Compounds

The transcendent purpose of heterogeneous photocatalysis is to decompose organic compounds that are harmful to humans and the environment. Photocatalytic oxidation processes (PCO) are able to replace many customary disinfection methods including ozonation, chlorination, and intense UV-C irradiation, which are potentially dangerous and often create biologically harmful

by-products. However, organic compounds that have successfully decomposed into CO_2 and harmless minerals by photocatalysis include phenols ,halophenols, haloalkanes, alkanes, aromatics, alcohols, polymers, surfactants, herbicides, pesticides, dyes, bacteria, viruses, fungi, molds, cancer cells, and highly resistant spores (Mills and Hunte, 1997). In addition to the strong oxidation characteristics of a PCO process, a second advantage it provides for environmental purification and disinfection purposes. Nanoparticle photocatalysts are easier to create high efficiency and can be implemented in mixed aqueous solutions.

2.3. Dyes and Their Treatment Methods

2.3.1. Dyes

A dye can generally be described as a coloring substance that has an affinity to the substrate to which it is being applied. The dye is generally applied in an aqueous solution, and may require a mordant to improve the fastness of the dye on the fiber. Both dyes and pigments appear to be colored because they absorb some wavelengths of visible light preferentially. In contrast, a pigment generally is insoluble, and has no affinity for the substrate. Coloration is a key factor in the commercial success of textile products, particularly those with high fashion content, especially garments, furnishings and upholstery. The business generated by the dye industry over the last two years was approximately US$ 22 billion, and constituted a total employment of about 1.45 million people. Excluding fluorescent brighteners, the dye consumption per capita is approximately 150 g per year, serving an average consumption of textile fiber of about 14.0 kg per year per inhabitant. Despite the high economic importance of the textile industry in the world, this industry is responsible for over 7×10^5 metric tons of about 10,000 different types of dyes and pigments produced each year. Among industries, responsible for pollution of the aquatic ecosystems textile dyeing and printing industries are major players. Around half of a ton of these dyestuffs are lost per day to the environment. Approximately 200 liters of water are required, for every kilogram of finished cotton fabric. The reactions necessary to fix these dyes to the fibers are not very efficient. Therefore, residual dyes, several types of chemicals and salts are dumped into the water and are discharged in the wastewater system. At least 15% un-used dyes might enter the environment through effluents from wastewater treatment plants (Carneiro *et al*., 2004).

2.3.2. Treatment of Dye Contaminated Water

Removal of color in wastewater generated by the textile industries is major issue of discussion and regulation all over the world. Among the dyes, the textile azo dyes with synthetic intermediates as contaminant and their degradation products have undoubtedly attracted the most attention with regard to their high environmental impact, because of their widespread use, their potentiality to form toxic aromatic products (carcinogenicity and mutagenicity properties) and their low removal rate during primary and secondary treatment. They represent about 50% of the worldwide production and correspond to an important source of contamination considering that a significant part of the synthetic textile dyes are lost in waste streams during manufacturing or processing operations. Therefore, it is important to develop effective wastewater remediation technologies for these compounds (Senthikumaar et *al.,* 2005).

Various chemical and physical treatment processes are currently proposed for these dyes. These dye treatment methods largely fall into the categories of direct precipitation or elimination by adsorption, flocculation, membrane separation, coagulation and chlorination (Dabrowski, 2001). These methods have largely been incomplete and ineffective because the dyes are not completely destroyed and require further treatment. A number of biological processes, such as sequenced anaerobic/aerobic digestion, have been proposed in the treatment of textile wastewater, but they are limited due to the fact that many of the dyes are non-biodegradable. Alternative methods based on advanced oxidation processes combining ultraviolet irradiation and oxidative agents for dye treatment have also been investigated, but the presence of intermediates arising from the photodegradation reaction could be more harmful than the pollutant itself (Robinson *et al*., 2001). Attention has earlier been focused on heterogeneous photocatalysis for the treatment of recalcitrant chemicals present in the wastewater. Among these heterogeneous photocatalysis in the presence of irradiated semiconductors (TiO_2, WO_3, SnO_2, ZnO, ZnS, CdS and others) and CdS in particular has been successfully used to decolorize and mineralize many organic pollutants including several dyes and their intermediates present in aqueous systems using both artificial light and under sunlight using solar technology (Muruganandham *et al*., 2005)

2.4. Methods of` Synthesizing CdS Nanomaterial

2.4.1. Precipitation Method

CdS:Mn powder samples were prepared by chemical route using their acetate salts. 2.6640 g of $Cd(CH_3COO)_2$ was completely dissolved in 100ml of methanol to form 0.1M solution and 2.9964 g of $Mn(CH_3COO)_2$ was completely dissolved in 100ml of methanol to form 0.1M solution. These two solutions were mixed in appropriate concentration to get the desired ratio of Cd:Mn and the solution was taken in a burette. Similarly 0.1M solution of Na_2S with a few drops of thiophenol was prepared and this solution was taken in a conical flask. Thiophenol was used as both reductant and surfactant. Now the solution in the burette is added drop by drop into conical flask under continuous stirring for about 6 hours until fine precipitate of yellowish CdS: Mn was formed. Then the precipitate was filtered out separately and washed thoroughly with de-ionized water to remove the by-product, sodium acetate salt. Finally these samples were calcined at 3000 ^0C for 2 h in vacuum to induce crystallinity, because the preliminary XRD studies on as prepared samples showed amorphous structure. A single step chemical reaction is given below for the precipitation of the Mn doped CdS nanoparticels

$$(1\text{-}x)CdCH_3COOH + xMnCH_3COOH + Na_2S \rightarrow CdS{:}Mn\downarrow + 2NaCH_3COOH$$

2.4.2. Incipient Wetness Impregnation Method

Incipient wetness impregnation is a commonly used technique for the synthesis of heterogeneous catalysts. Typically, the active metal precursor is dissolved in an aqueous or organic solution. Then the metal-containing solution is added to a catalyst support containing the same pore volume as the volume of solution that was added. Capillary action draws the solution into the pores. The catalyst can then be dried and calcined to drive off the volatile components within the solution, depositing the metal on the catalyst surface.For example Co/SiO_2 was prepared using a cobalt nitrate-impregnating solution containing four moles of citric acid (Aldrich, 99.5%) per

gram atom of cobalt. After impregnation, samples were dried at 120 ^{O}C and then heated at 450 ^{O}C for 4 h in ambient air (Baatz *et al*., 2008).

2.5. Approaches for Making Cadmium Sulfide Visible Light Active

The recombination of photo generated electrons and holes are believed to be reason for the low photoactivity of semiconductor photocatalysts. In order to enhance the semiconductor photocatalysis as well as the response into the visible spectrum of solar light, the photocatalyst has to be doped with certain transition metals, non-metals and ionic components. Doped ions can also act as charge trapping sites and thus reduce electron-hole recombination. The effect of doping on the activity of photocatalyst is governed by several factors, e.g. the type and concentration of dopant, preparation method, the structure and the initial concentration of the pollutants (dyes and phenols), physico-chemical properties of the catalyst. Both positive and negative results have been reported from doping with metal ions. The increase in charge separation efficiency will enhance the formation of both free hydroxyl radicals and active oxygen species (Kato *et al*., 2005). There are different methods for making cadmium sulfide active in visible light thereby increasing its photocatalytic activity. Some of the major methods are discussed in this section.

2.5.1. Metal doping

The number and the life time of electrons/holes are particle size and dopant dependent. The photodegradation of dyes (5 mg/L) were studied in the presence of ZnS:Mn (2-10 %), ZnS:Ni (2-10%) and ZnS:Cu (2-10 %) for the degradation of methylene blue and safranin (Pouretedal *et al.,* 2009). In the study made by the above authors, metal doped ZnS showed beeter photocatalytic activity as compared to the undoped ZnS.

2.5.2. Co-doping

2.5.3. Metal-Metal co-doping

Lu *et al*. (2009) evaluated the photocatalytic property of La and Nd co-doped CdS for degradation of unsymmetrical dimethyl hydrazine under UV light irradiation. It was found that Nd and La doped CdS have better photocatalytic activity than undoped CdS for degradation of unsymmetrical dimethyl hydrazine. Using CdS photocatalyst doped with La 2% (at), Nd 2.5% (at), La 2% (at) Nd 1.5% (at), the degradation rate of unsymmetrical dimethylhydrazine was reached 83%, 91%, 97%, respectively by catalyst of 0.1 g/L in 100 min at room temperature.

According to these authors, the effect might be due to the synergic operation of the two dopants in trapping charge carriers and mediating interfacial charge transfer process. Co-dopant of La^{3+} and Nd^{3+} could effectively inhibit the recombination of the photo induced electrons and holes. Nanocrystalline CdS co-doped with La^{3+} and Nd^{3+} at optimal concentration (2% (at) La^{3+} and 3% (at) Nd^{3+}) shows a better synergistic effect, which significantly increases the photodegradation activity of pure CdS. The separation of the charge carriers is attributed to such trappings. The co-doped CdS photocatalysts with appropriate content of La^{3+} and Nd^{3+}possessed abundant electron traps so as to be favorable for the separation of the photo induced electron-hole pairs, which could greatly enhance the activity of the photocatalysts.

2.6. Effect of Parameters on Photocatalytic Process

In photocatalytic degradation the followings are operating parameters which affect the process: pH of the solution to be degraded, and the pH of the precursor solution (catalyst's solution during preparation of catalyst); effect of dye concentration and effects of amount of catalyst. These parameters will be considered one after the other as they influence the photocatalytic processes of the degradation of dyes in waste waters.

2.6.1.Effect of pH

PH of the solution also affects the rate of photodegradation of the dye by changing the surface charges of the nanophotocatalyst particles. Hence adsorption of charged particle at the surface of catalyst is altered which changes the rate of degradation reaction. Photocatalyst surface may protonate or deprotonate with the change of pH value. Anionic dyes will be degraded more at lower pH. Reductive cleavage may take place in azo dyes at low pH favoring the degradation of azo dyes (Soutsas *et al*., 2010).

Organic compounds in wastewater differ greatly in several parameters, particularly in their speciation behavior, solubility in water and hydrophobicity. While some compounds are uncharged at common pH conditions typical of natural water or wastewater, other compounds exhibit a wide variation in speciation (or charge) and physico-chemical properties. At pH below its pKa value, an organic compound exists as a neutral species. Above this pKa value, organic compound attains a negative charge. Some compounds can exist in positive, neutral, as well as negative forms in aqueous solution. This variation can also significantly influence their

photocatalytic degradation behavior. pH of the wastewater can be varied significantly. pH of aquatic environment plays an important role on the photocatalytic degradation of organic contaminants since it determines the surface charge of the photocatalyst and the size of aggregates it forms (Bahnemann and Haque, 2007). The surface charge of photocatalyst and ionization or speciation (pKa) of an organic pollutant can be profoundly affected by the solution pH. Electrostatic interaction between semiconductor surface, solvent molecules, substrate and charged radicals formed during photocatalytic oxidation is strongly dependent on the pH of the solution. In addition protonation and deprotonation of the organic pollutants can take place depending on the solution pH. Sometimes protonated products are more stable under UV irradiation than its main structures (Saien and Khezrianjoo, 2008). Therefore, the pH of the solution can play a key role in the adsorption and photocatalytic oxidation of pollutants.

2.6.2. Effect of Dye Concentration

The quantity of the dye adsorbed on the surface of the photocatalyst is of foremost importance since only this amount contributes to photocatalytic process and not the one in the bulk of the solution. The extent of dye adsorption depends on the dye initial concentration. Generally speaking the percentage degradation decreases with increasing amount of dye concentration, while keeping a fixed amount of catalyst (Wang *et al*., 2008). Using ZnO, Pardeshi and Patil (2009), tested the effect of initial concentration (50-300 ppm) on the photocatalytic degradation of resorcinol under solar light. The degradation efficiency in 7 h decreases from 100 to 43.8% as the initial concentration increases from 100 to 300 ppm.The auther examined the effect of initial substrate concentration (2 - 5 g/l) on the photocatalytic degradation of phenol under sunlight, visible and UV light,respectively. With the increase in the substrate concentration, the degradation efficiency decreased from 100% to 60% under solar irradiation. Under UV light, the degradation was reported to decrease from 94% to 52% with increasing initial concentration. The degradation was found to decrease from 95% to 50% under visible light.

2.6.3. Effects of Amount of Catalyst

Heterogeneous photocatalysis is influenced by the concentration of photocatalyst. $^{\bullet}OH$ radicals are increased with the increase in concentration of photocatalyst resulting decolorization of the dye. After a certain limit of time concentration of catalyst solution become opaque and light

radiation cannot enter in to activate the catalyst particles. Hence the rate of dye degradation will be decreased (Sun *et al.,* 2008).

2.6.4. Point of Zero Charge (PZc) of Photocatalysts

The ionization state of the surface of the photocatalyst can be protonated and deprotonated under acidic and alkaline conditions respectively as shown in the following reactions:

$$pH<Pzc \quad TiOH + H^{+} \rightarrow TiOH_2^{+} \quad (2.1)$$

$$pH>Pzc \quad TiOH + OH^{-} \rightarrow TiO^{-} + H_2O \quad (2.2)$$

The point of zero charge (PZc) of the TiO_2 (Degussa P25) is reported at pH~6.25 (Zhu *et al.,* 2005). Under acidic conditions the positive charge of TiO_2 surface increases as the pH decreases (Eq.2.1); above pH 6.25 the negative charge at the surface of the TiO_2 increases with increasing pH. Moreover, the pH of the solution affects the formation of hydroxyl radicals by the reaction between hydroxide ions and photo-induced holes on the TiO_2 surface. The positive holes are considered as the major oxidation steps at low pH, whereas hydroxyl radicals are considered as the predominant species at neutral or high pH levels (Shifu and Gengyu, 2005). It would be expected that the generation of $OH^{\bullet}$ radicals are higher due to the presence of more available hydroxyl ions on the TiO_2 surface. Thus the degradation efficiency of the process will be logically enhanced at high pH. The degree of electrostatic attraction or repulsion between the photocatalyst's surface and the ionic forms of organic molecule can vary with the change in solution pH, which can result in enhancement or inhibition on the photocatalytic degradation of organic pollutants in the presence of TiO_2. In the presence of P25 and ZnO, the effect of pH on the photocatalytic degradation of 4-fluorophenol was observed to be pH7 > pH9 > pH4 (Selvam *et al*., 2007).

As reported by Venkatachalam *et al*., (2007), the degradation rate of 4-CP was faster in the acidic pH range compared to the alkaline pH which was attributed to enhanced adsorption of 4-CP on the surface of nano TiO_2. Minimization of electron-hole recombination in the acidic pH was also

indicated to be an important factor for the enhancement of degradation. Mahmoodi and Arami, (2009), tested the effect of pH (3.5-10.5) on the photocatalytic degradation of Acid blue 25. Under the conditions examined, the optimum pH was reported to be 10.5 for the degradation of Acid blue 25. Using ZnS, Cun *et al*., (2002) examined the influence of pH (4.22-12.57) on the photocatalytic degradation of MO and noticed an optimum pH of 4.2. The ionization state of the surface of CdS photocatalyst can be protonated and deprotonated under acidic and alkaline conditions respectively as shown in the following reactions:

$$pH<Pzc \qquad CdSH + H^{+} \rightarrow CdSH_2^{+} \qquad (2.3)$$

$$pH>Pzc \qquad CdSH + OH^{-} \rightarrow CdS^{-} + H_2O \qquad (2.4)$$

3. MATERIALS AND METHODS

3.1. Experimental Site

The synthesis of nanosized CdS and Mn-Fe codoped,nanomaterials as well as the photocatalytic experiments and partial characterization of the as-synthesized nanomaterials by Uv-vis instruments were carried out at Haramaya University,Chemistry Department research laboratory.Where as the X-ray diffraction (XRD) patterns of the nanomaterials were determined done at Adama Science and Technology University(ASTU),Ethiopia.

3.2. Materials and Apparatus

3.2.1. Apparatus and Equipment

Some of the instruments and apparatus used for the study include: XRD, UV/Visible spectrophotometer, reactor tube, analytical balance, pH meter, hot plate, furnace, ceramic crucible, agate mortar, centrifuge, water bath, thermometer, volumetric flasks, pipettes, graduated cylinders, desiccators, magnetic stirrer, test tubes, and beakers.

3.2.2. Reagents and Chemicals

In the preparation of CdS and Fe-Mn codoped CdS the following chemicals were used: cadmium nitrate ($Cd(NO_3)_2.4H_2O$, MW: 308.48g/mol, Assay 99%, standard line chemical limited Mumbai 400102), $Cd(NO_3)_2.9H_2O$, 341g/mol, sodium sulfide ($Na_2S.\ 9H_2O$, MW: 240.18 g/mol, Min. Assay 99%, BDH (England)), Sodium hydroxide (NaOH, MW 40 g/mol, 99.0%, FLUKA (Switzerland)), hydrochloric acid (HCl, MW: 36.5 g/mol, Min Assay 99.0%), Ferric nitrate ($Fe(NO_3)_3$, MW: 404 g/mol, Min Assay 98%, BLULUX), Sodium nitrate ($NaNO_3$),Glycine, 1-Butanol ($CH_3(CH_2)_2CH_2$-OH, MW: 74.12 g/mol, Min Assay 99%, BLULUX), n-Hexane ($CH_3(CH_2)_4CH_3$, MW: 86.18 g/mol, Min Assay 99%, BLULUX), Ethanol (CH_3CH_2OH, MW: 46.08 g/mol, 99.4% by volume, Lab tech chemicals), cetyltrimethyl ammonium bromide (CTAB) ($C_{19}H_{42}Br$, MW: 364.46 g/mol, Min Assay 98%, BDH (England)) and distilled water. All chemicals and reagents were purchased and used without further purification.

Methylene blue $C_{16}H_{18}N_3SCl$, MW 319.50 g/mol. The structure of Methylene blue is given below:

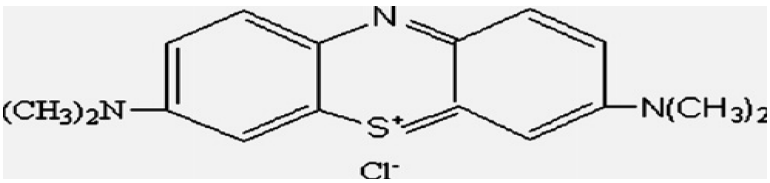

Figure 1 structure of methylene blue

3.3. Methods of Synthesis and Characterization

3.3.1. Synthesis of CdS Nanoparticels

The aqueous solution of cadmium nitrate (0.1M) was added to solution of sodium sulfide (0.1M) in round bottom flask and stirred for 15 h. The resultant mixture was heated at temperature <100 ^{0}C for several hours and then filtered off. The residue obtained after the heating was dried in an oven and then calcined at 600 ^{0}C in a programmable furnace. The yellow reaction mixture obtained as such was allowed to evaporate at room temperature which resulted finally to the yellow colored solid of CdS nanoparticles (Ravikant. *et al*., 2012).

3.3.2. Synthesis of Fe-doped CdS Nanoparticels

Fe-doped CdS was synthesized by mixing 50 mL of 0.2 M $CdCl_2$, 10 mL of 0.2 M $FeCl_3$ and 50 mL of 0.2 M $Na_2S{\cdot}9H_2O$ solutions. The mixture was stirred at 80 ^{O}C using magnetic stirrer and in to this mixture 100 mL of ethanol was added with further stirring. After adding 15 mL of deionized water drop by drop, the stirring process was continued further for 2 h. Following this, the mixture was cooled at room temperature for the precipitate to settle out. The precipitate so formed have been dried in an oven at 80 $^{\mathbf{o}}$C for 24 h and then calcined at 500 ^{O}C for 2 h. Finally the sample was grinded in agate mortar and labeled as iron-doped cadmium sulfide (Iorgu *et al.*, 2013).

3.3.3. Synthesis of Mn doped CdS Nanoparticels

With a doping concentration of 10% (mol), Mn-doped CdS was prepared by the incipient wetness impregnation method. Accordingly,2.214 g of manganese nitrate nonahydrate [$Mn(NO_3)_2{\cdot}9H_2O$]

was dissolved to 100 mL of deionized water and then 10 g of undoped CdS was added and the mixture was stirred continuously for 1 h. The precipitate so formed was allowed to settle down for 24 h, filtered with 0.2 μm membrane filter and washed three times each time with deionized water and ethanol. The filtered precipitate was dried at 105 ^{O}C for 12 h. After drying it properly the resulting solid was calcined at 550 ^{O}C for 2 h in a programmable furnace. The product so obtained was labeled as manganese-doped CdS. **(**Venkatesu and Ravichandran, 2012).

3.3.4. Preparation of Fe and Mn Co-Doped CdS Nanoparticels

In a typical synthesis, 5 g of the as synthesized Fe-doped CdS nanoparticles was transferred to a ceramic crucible and 5mL of $Mn(NO_3)_2.9H_2O$ solution (0.18 M) was added into it. After agitating with glass rod, the crucible with its content was transferred to an oven for drying at 110 ºC for 30 min. The resulting dried powder was calcined at 600 °C, cooled to room temperature, ground in an agate mortar and then labeled as Fe-Mn CdS codoped nanocomposite.

3.4. Methods of Characterization

3.4.1. Determination of X-ray Diffraction (XRD) Patterns

X-ray diffraction patterns of the as-synthesized photocatalysts was obtained using X-ray Diffractometre (XRD) BRUKER D8 Advance XRD, AXS GMBH, and Karlsruhe, West Germany) equipped with a Cu target for generating a Cu Kα radiation (wavelength 1.5406 A°) at Adama University (AU). The measurement was carried out at room temperature, and the accelerating voltage and the applied current was set to 40 kV and 30 mA, respectively. The instruments were operated under step scan type with step time and degree (2θ) of 1s and 0.020°, respectively over the range: 4° to 75°.

3.4.2. UV-Vis Diffuse Absorption Edge Determination

For the estimation of absorption edge of the as-synthesized photocatalysts, the UV–Vis diffuse absorption was measured using SP65 spectrophotometer at Haramaya University research laboratories by scanning over the wave length range of 200 - 800 nm.

3.5. Photocatalytic Degradation Experiment

3.5.1. Reactor Design for Photo Degradation Studies

The photocatalytic efficiency of as-synthesized nanomaterials for the degradation of methylene blue dye was investigated under visible light irradiation. Effects of variables such as photocatalyst

dosage (0.05–0.15 g/L), initial MB concentration (10–50 mg/L) and pH (2.0–12) were studied. The experiments were conducted by changing one variable at a time while keeping other parameters constant. All photocatalytic degradation experiments were carried out in duplicate at room temperature. A known amount of the as-synthesized photocatalyst powder was mixed with the dye solution in a reactor tube. This mixture was stirred first in dark for 30 min to obtain adsorption-desorption equilibrium before illumination. During the illumination of the sample by visible light radiation, air was purged into the solution with the help of porous tube. For the absorbance measurement, 10 ml of the mixture was withdrawn at 20 min interval of time, centrifuged at 2500 rpm for 5 min and filtered to remove the catalyst particles. Finally, the absorbance of the clear solution was recorded at the maximum absorption wave length (λ_{max} = 661 nm) of the dye using UV/Vis spectrophotometer and this was used for the purpose of quantitative analysis of the samples. All photocatalytic degradation experiments were monitored spectrophotometrically by using Mn-Fe codoped CdS as a photocatalyst.

(a) Reactor tube made of pyrex glass containing the reactants

(b) Inlet tube for air purging

(c) Outlet for collecting sample at regular interval

(d) Radiation source

(e) Magnetic stirrer

Figure 2.Diagrammatic representation of the Photocatalytic reactor

Percent degradation of methylene blue dye was calculated by the following formula:

Where, C_o is initial dye concentration, C_t is the concentration of dye at irradiation time t, A_o is dye initial absorbance before Visible light irradiation and A_t is the absorbance of dye at irradiation time t.

3.5.2. Factors Affecting Photocatalytic Degradation of Dye

3.5.2.1. Effect of Concentration of Methylene Blue

The effect of methylene blue concentration on the rate of its photocatalytic degradation was studied by taking different concentrations (10 mg/L to 50 mg/L) of methylene blue.

3.5.2.2. Effect of pH of the Solution

The effect of pH on photocatalytic degradation of methylene blue was investigated over the pH range of 2 to 12 (Pouretedal *et al*., 2009 ; Xu.X et al.,2004) . The pH was maintained using 1 M HCl or 1 M NaOH measured using a pH meter (Mettler Toledo MP220).

For CdS, the pH of the point of zero charge (pH_{pzc}) was found in the 6.9 to 9.8 range (Sedlak and Janusz, 2008). This was performed by the following procedure. MB (100 mL) prepared by mixing (10-50 mg/L) with untreated Fe-Mn codoped CdS at a dose of 0.2 g .

3.5.2.3. Amount of Photocatalyst

The effect of amount of photocatalyst on the rate of photocatalytic degradation of methylene blue was determined by taking different amounts of Fe and Mn co-doped CdS (50 to 250 mg/L) keeping other factors constant (P^H,concentration of dye).

4. RESULTS AND DISCUSSION

4. 1. Characterization of Photocatalysts

4. 1. 1. UV/Vis spectrophotometric results of photocatalysts

Optical study of undoped and Fe-Mn codoped CdS nanoparticles was conducted by using UV/Vis spectrophotometer (Model: NOVA 1100 AVR). For the measurement of UV/Vis absorbance, 0.1 g of each powdered sample was dispersed in distilled water. The suspension was taken into cuvet made of quartz glass and optical absorbances of CdS, Mn-CdS, Fe-CdS and Mn- Fe codoped CdS nanoparticles were recorded with a scan speed of 333 nm/min in the range of 200-800 nm. Fig 3.shown below presents the absorption spectra of CdS, Fe-CdS and Fe-Mn Codoped CdS nanoparticles. The corresponding absorption peak of CdS, Fe-CdS, and Fe-Mn Codoped CdS are observed at about 400 nm, 429 nm and 496 nm respectively. All the nanoparticles showed broad peaks and these absorption bands are red shifted with respective to that of the corresponding bulk compound (515 nm) that is CdS, asserting the formation of nanosized particles and thus in agreement with the findings reported by Thambidurai *et al*., (2013).

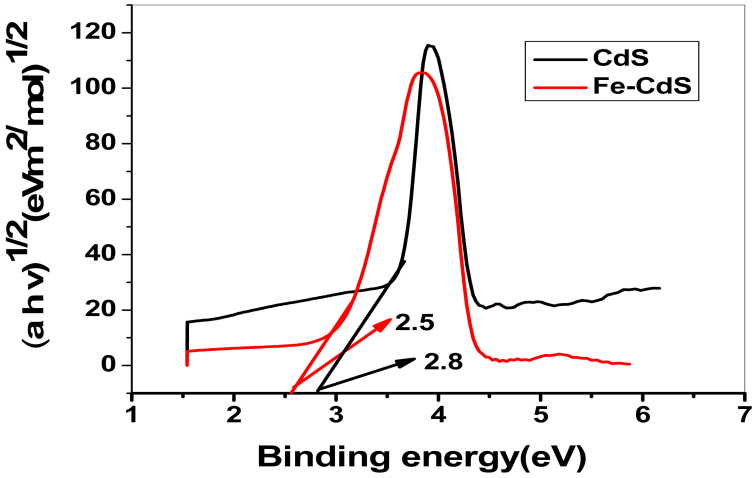

Figure3.Uv/Vis Absorption spectra of CdS,Fe:CdS,and Fe,Mn:CdS nanoparticles

The bang gap energy *(E_g)* of the photocatalysts was calculated using the equation:

$$Eg = 1240/\lambda_{max},$$

Where, E_g is band gap energy in electron volts, and λ_{max} is the wavelength (nm) at maximum absorbance and 1240 is a constant obtained from hν.

The calculated band gap energies so obtained for the undoped CdS, Fe-CdS and Fe-Mn Co doped CdS nanoparticles are found to be 2.8 and 2.5 eV, respectively. The red shifting of the absorption peaks in the three samples is the result of decreasing band gap with the longer wave length of excitation. In general the band gap of a semiconductor becomes smaller with decreasing particle size, and is indicated by an absorption shift to longer wave lengths. This means that the levels of the valence band are moderately shifted to lower energies, while those of the conduction band are strongly shifted to higher energies.

4.1.2 XRD analysis result of photocatalysts

The XRD patterns of Calcined CdS,Fe-CdS,Mn-CdS and Fe-Mn codoped CdS are shown in Figures-4 A,B,C and D respectively. The observed diffraction peaks at 2θ values of 24.9º, 26.5º, 28.2º, 36.7º, 43.8.º, 48.0º, 51.0º, 52.9º, 54.7 º and 66.6º for undoped CdS correspond to the Bragg planes (1 0 0), (0 0 2), (1 0 1), (1 0 2), (1 1 0), (1 0 3), (2 0 0), (1 1 2), (0 0 4) and (2 0 3) respectively. The peak at 26.565º is the characteristic of CdS cubic phase. It is diffracted from (1 0 0) plane of the product. The other peak at 24.9º diffracting from (0 0 2) is the characteristic of CdS hexagonal phase.

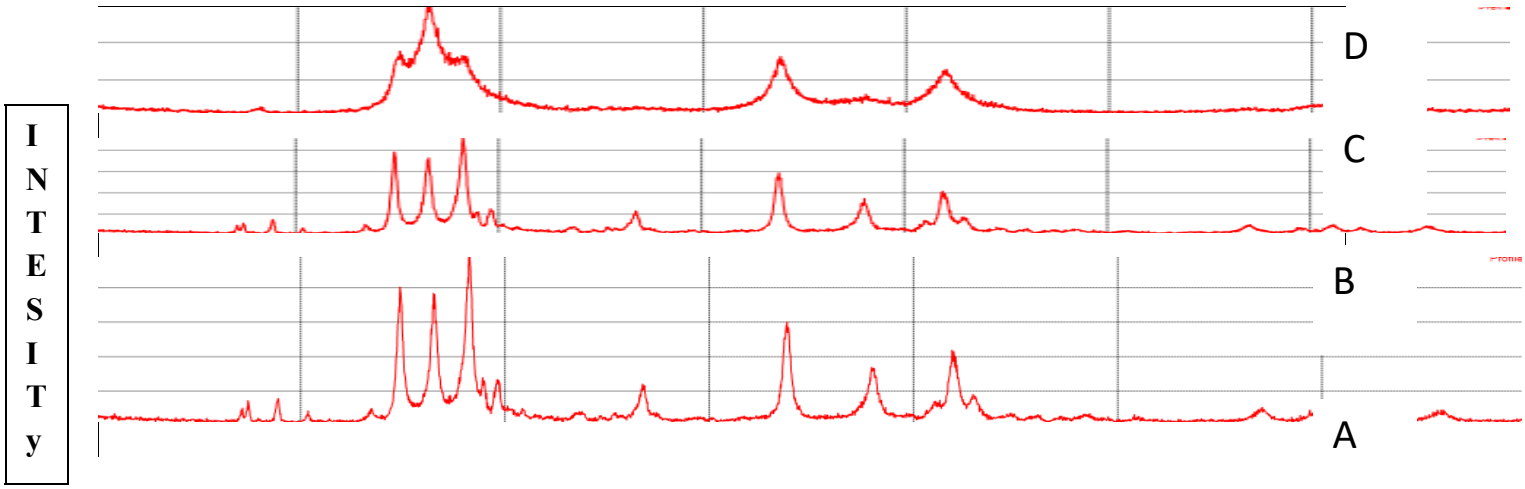

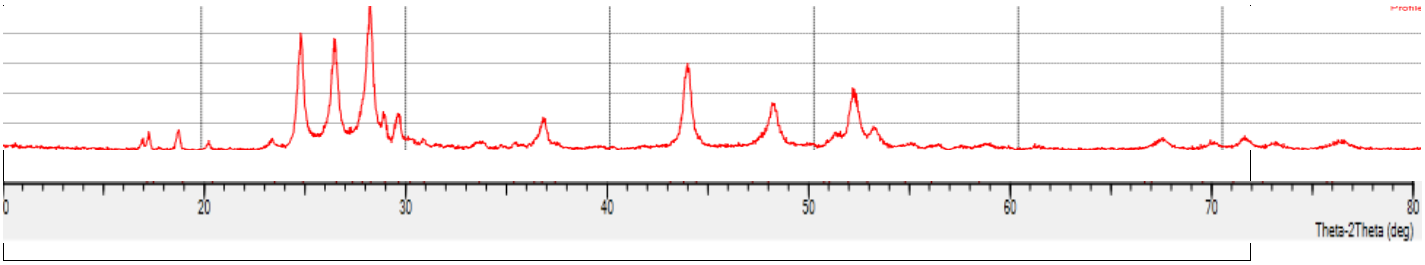

Figure 4. X-ray diffraction patterns of (D) Fe-Mn codoped CdS (C)Fe-CdS (B) Mn-CdS (A) CdS nanoparticles.

The average crystallite size (D) corresponding to each of the as-synthesized nanoparticles was calculated by using Scherrer's formula, $D = 0.94\lambda/\beta\cos\theta$, where λ is the wavelength of X-ray used (0.154 nm), β is the full width at half maximum (FWHM) and θ is the Bragg angle (is the degree of the diffraction peak with geometric factor 0.94).

The result is indicated in table 1, and the values of D were found to be 21.0 nm, for undoped CdS, 20.1 for Fe-doped CdS, 18.17 for Mn-CdS and 16.63 nm, for Fe-Mn Codoped CdS nanoparticles.

Table 1.Average crystallite size (D) of as-synthesized photocatalysts

Sample	2Θ (degree) ±	β (radian) ±	d (nm) ±
CdS	28.2699	0.0068404	21.0
Fe:CdS	28.2688	0.007114	20.1

Mn: CdS	28.2649	0.00787	18.2
Fe,Mn: CdS	26.6042	0.008568	16.6

4.1.3. Point of Zero Charge (PZc) of Photocatalysts

The PZC is a condition where the surface charge of the photocatalyst is zero or neutral that lies in the pH range of 1-14 depending on the catalysts used. Figure 5.Show the plot of point of zero charge of Fe-Mn codoped CdS at 6.1. At this PZC of the as-synthesized photocatalysts,it is assumed that the interaction between the photocatalyst particles and water contaminants is minimal due to the absence of any electrostaticforce. Accordingly, the photocatalytic activity of Fe-Mn Codoped CdS was maximum (79.5 %) when the working solution was at pH 4 < (PZc) and slightly decreased in percent degradation (67.4 % to 33.2 %) with increasing the pH (4-11) of the solution. When operating at pH < PZc, the surface charge for both CdS and Fe-Mn Codoped CdS becomes positively charged and gradually exerted an electrostatic attractive force towards the negatively charged MB dye. Such polar attractions between charged anionic organic compounds and the positively charged photocatalyst surfaces and make it easy can intensify the adsorption of water contaminants onto the photon activated photocatalyst surfaces for subsequent photocatalytic reactions (Xu and Langford, 2000). This is particularly significant when the anionic organic compounds are present at a low concentration level.

At pH > PZc, the catalyst surface would become negatively charged and repelled any anionic compound in water. At pH = PZc, the neutral surface charge of the catalyst particles is unable to produce any electrostatic interactive forces on the solution particles leading to a solid-liquid separation. Thus, this induces an aggregation of the catalyst whereby it becomes larger, leading to catalyst sedimentation (Blanco *et al*., 2001).

Figure 5. point of zero charge of l doped CdS Photocatalysts pH_f

4.2. UV-Visible Absorption Spectra of MB dye

UV-visible absorption spectra of the MB dye was shown in Figure 6. Two peaks are observed, one in the UV range at λ = 300nm and the other is in the visible range at λ =661 nm. All

spectroscopic measurement the dye concentrations were carried out at λ_{max}=661nm.

Figure 6 UV-Visible spectrum of MB dye

4.3. Photocatalytic Degradation Study of MB dye

4.3.1 Comparison of photocatalysts

Photocatalytic activities of the as-synthesized CdS, Fe- CdS, Mn-CdS and Fe-Mn Codoped CdS nanoparticles under visible light irradiation for the degradation of MB dye were evaluated and compared. Absorbance and percentage degradation of MB as function of time under visible radiation are given in Appendix Table 2. Figure7.shows the percentage degradation of MB dye in solutions with the same dye initial concentrations of 10 mg/L of MB with the same amounts (150 mg/L) of the photocatalysts CdS, Fe-CdS, Mn-CdS and Fe-Mn Codoped CdS nanoparticles

under visible light irradiation. The results show that,CdS has the least photocatalytic activity under visible light irradiation as compared with the rest. This may be due to the ability of the doped metals to trap electrons from CB. This process reduces the e^- and h^+ recombination at the CdS surface. Therefore, a more effective electron and hole transfer occurs to the electron acceptors and electron donors respectively and thus adsorbed on the surface of the particle than in the case of CdS.

The degradation or decolorization efficiencies of MB solutions under visible light irradiation using CdS, Fe-CdS, and Mn-CdS as photocatalysts were 69.4%, 72.6% , and 75.6% respectively over the time of 2h. Photocatalytic degradation of MB at 2 h using Fe-Mn codopedCdS nanoparticle as photocatalyst under visible light irradiation was as high as 79.5%. Because in Fe-Mn codopedCdS nanoparticle, there is efficient charge separation of electron and hole pairs in the excited states that prevents recombination of charge pairs for a longer time than single dopant under visible

radiation (Olad and Nosrati,

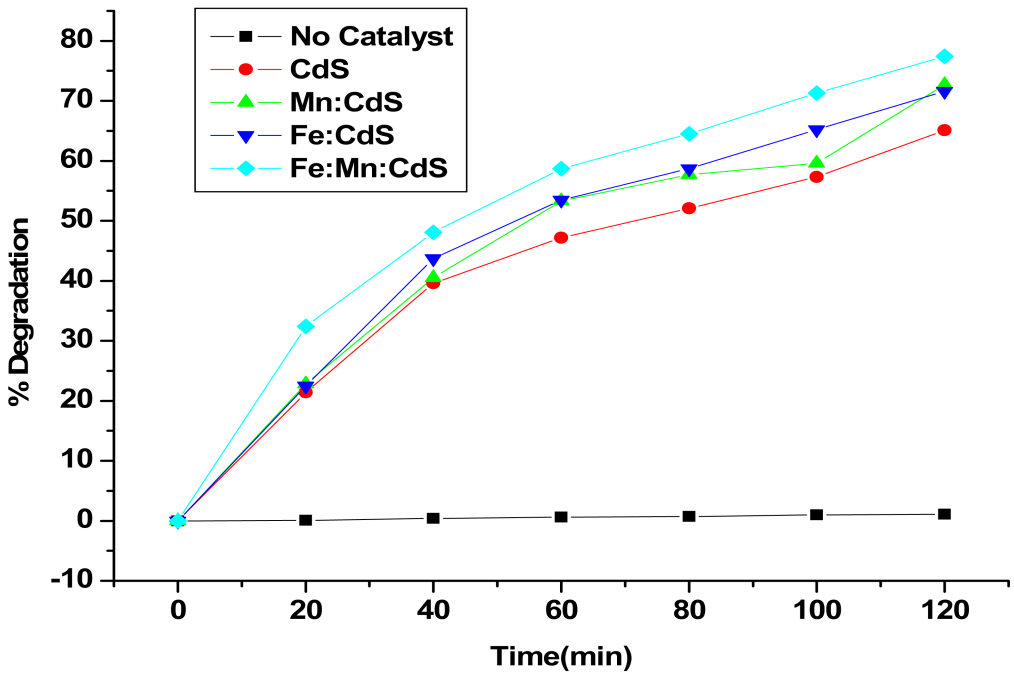

2011).

Figure7. Plot of % degradation of MB as function of time using CdS,Fe-CdS, Mn-CdS and Fe:Mn-Co doped CdS photocatalysts (MB = 10 mg/L ,and Fe,Mn:CdS =150 mg/L, pH = 4)

4. 4. Factors Affecting the Photocatalytic Degradation of Methyl Blue

4. 4. 1. Effect of pH

Literature review revealed that pH plays a significant role in the degradation of dye solution and this could show a significant variation in its effect for different ranges (Oturan *et al*., 2008). The samples of the reaction mixture at different pH were studied and maximum percentage degradations of MB at different pH values were found to be 61.9%, 43.0%, 39.1 %, 37.0 %, 35.2% and 22.4% at pH 4, 6, 8, 10, 2, and 11, respectively. Hence, Fig.8. shows that the degradation of MB was greatly influenced by pH of the dye solution. The strong effect of pH on the photodegradation efficiency of MB solution was observed at pH of 4. The pH affected surface binding sites of the adsorbent (due to anionic dye solution) as well as the availability of the adsorbate compound (due to cationic photocatalyst). When operating at pH < PZc, the surface charge for CdS and Fe-Mn:Codoped CdS becomes positively charged and gradually exerted an electrostatic attractive force towards the negatively charged MB dye. Such polar attractions between charged anionic organic compounds and positively charged photocatalyst surfaces can intensify the adsorption of water contaminants onto the photon activated photocatalyst surfaces for subse

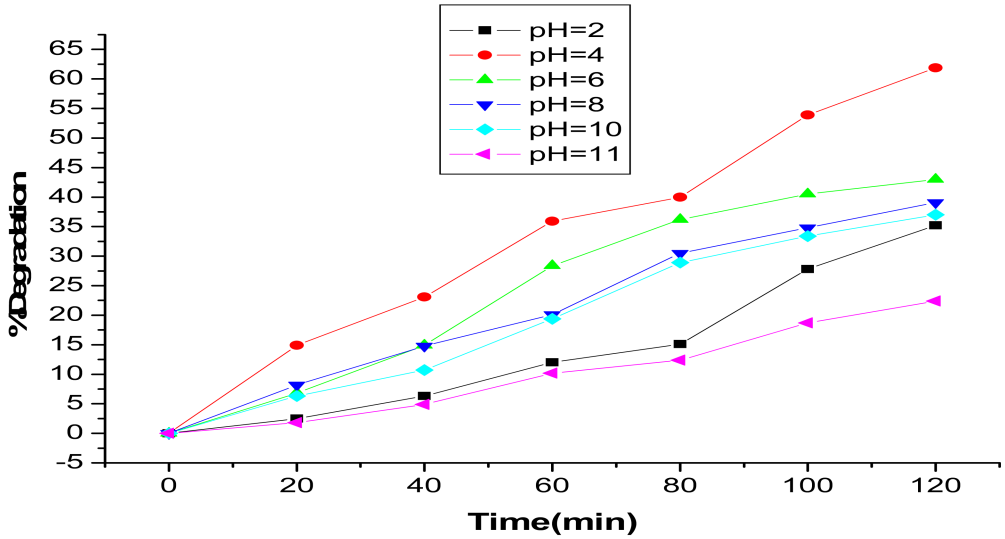

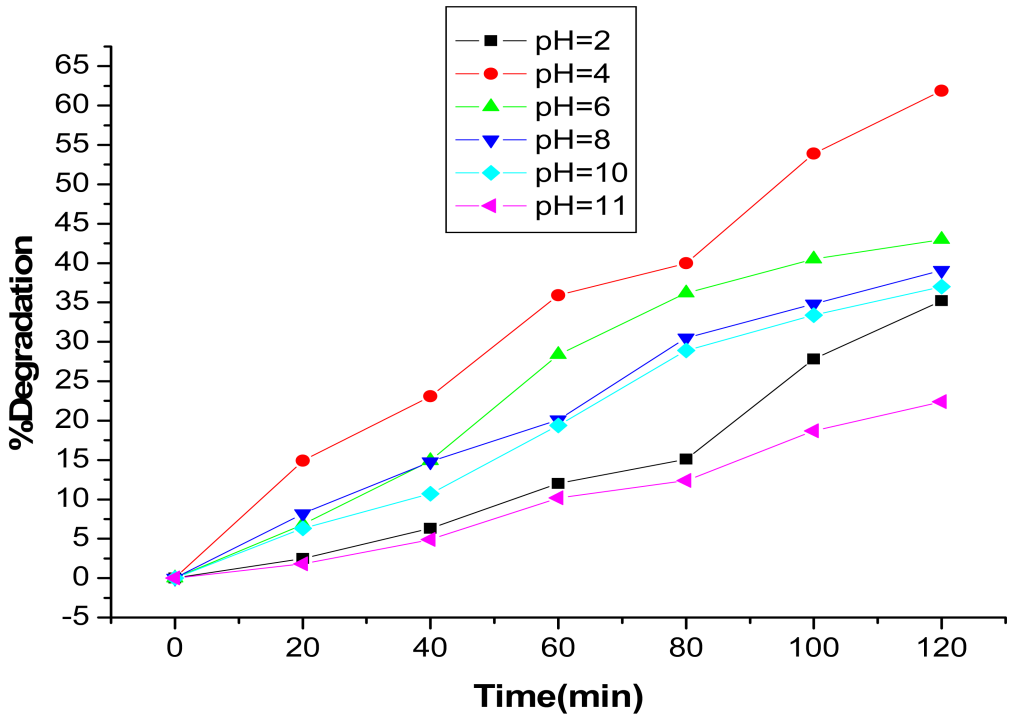

Figure 8. Plot of percent degradation of MB as function of time by varying the pH of the solution keeping both dye and photocatalyst amounts constant (MB = 10 mg/L ,and Fe-Mn:CdS =150 mg/L)

4.4.2 Effect of catalyst loading

The amount of photocatalyst is one of the main parameters for the degradation of substrate from economical point of view. In order to avoid the use of excess photocatalyst, it is necessary to find out the optimum loading of photocatalyst for efficient removal of dye (Sakthivel *et al*., 2003). Hence, a series of experiments were carried out to find the optimum amount of the photocatalyst Fe-Mn:CdS by varying its amount from 50-250 mg/L. The percent degradation of dye versus time of degradation by varying the photocatalyst weight is recorded in Appendix Table 4 and the corresponding plot is given in Figure 9. To achieve highest photocatalytic reaction rate, from the plot the optimum amount of the photocatalyst was found to be 150mg/L. Upon increasing the amount of photocatalyst up to 150mg/L percent of degradation increases due to the increase in the adsorbent total surface area and thus, the number of active sites, available for the

photocatalytic reaction. However, excess photocatalyst, above this optimal load, would induce more aggregation (particle–particle interactions) of photocatalyst making a significant fraction of the catalyst inaccessible either to the adsorbing dye or to the radiation (Wong and Chu, 2003). The degradation efficiency decreases after achieving an optimum value of photocatalyst load. Therefore, 150mg/L of the photocatalyst was selected as the optimal amount of photocatalyst for the subsequent experiments.

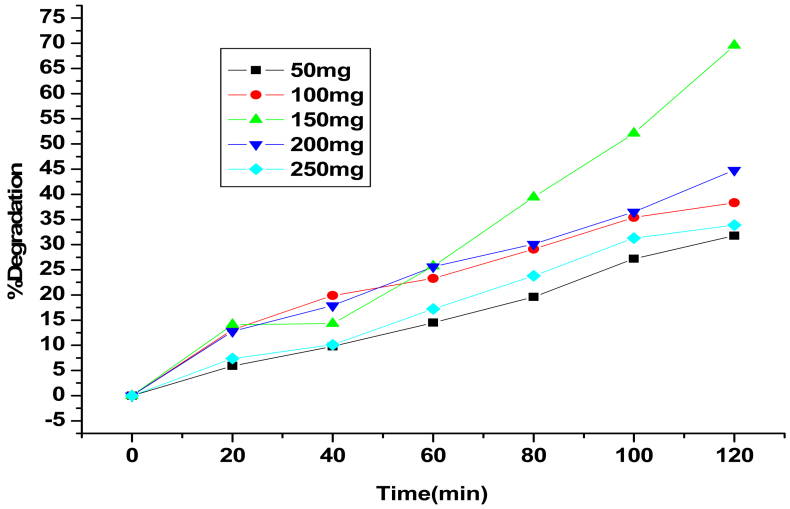

Figure 9.plots of % degradation of MB versus time by varying the amount of Fe-Mn CdS photocatalyst(pH = 4, 10 mg/L MB and λ_{max}= 661 nm).

4.4.3 Effect of initial concentration on the photocatalytic degradation of MB dye

The effect of the substrate initial concentration on the degradation of MB was studied at different concentrations of dye by varying it from 10 mg/L to 50 mg/L and keeping the photocatalyst load at 150mg/L. The percentage degradation of MB at different concentrations as a function of time under visible radiation is given in appendix table 5. Figure10. Shows the percentage degradation of MB in solutions with the same amount of Fe-Mn:CdS photocatalyst (150 mg/L). The highest (maximum) degradation was found to be at 10mg/L initial concentration of MB. As the dye concentration is increased and the catalyst amoussssssnt kept constant, fewer active sites would be available per substrate (dye) to interact with. Thus,resulting in decreased rate of photocatalytic degradation (Davis *et al*., 1994,). Furthermore, at higher dye initial concentration, the approach of

the radiation photons to the catalyst surface is hindered and screened off, thereby, reducing the photocatalytic activity in the system (Epling and Lin, 2002). Moreover, at the higher dye concentration, the number of collisions between dye molecules increases at the cost of required collisions between dye molecules and **.**OH radical and therefore, the rate of reaction is retarded (Lodha*etal*,2008).

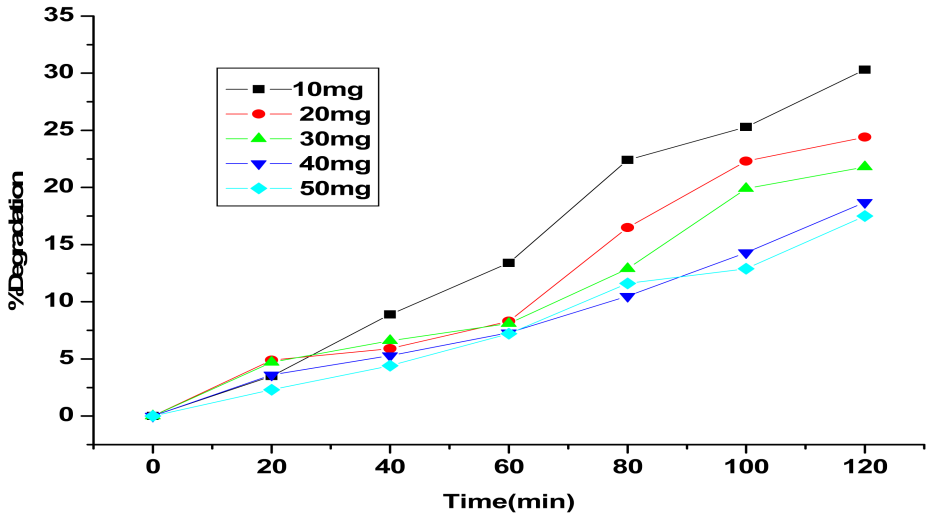

Figure 10. Plots of % degradation as function of time under visible light irradiation by keeping the Fe-Mn:CdS photocatalyst load constant and varying the amount of MB solution (Fe-Mn:CdS =150 mg/L, pH = 4 and λ_{max} = 661 nm).

5. SUMMARY AND CONCLUSION

In this study,cadmium sulfide (CdS), iron doped cadmium sulfide (Fe-CdS), and Fe-Mn codoped CdS nanoparticles were synthesized via preciptation method. The nanostructures of the prepared

CdS, Fe-CdS, Mn-CdS and Fe-Mn codoped CdS nanoparticles were confirmed using UV/Vis absorption and X-ray diffraction analysis. From XRD analysis, the average crystallite sizes of the as-synthesized CdS,Fe-CdS,Mn-CdS and Fe-Mn codoped CdS nanoparticles were found to be 21.0 nm, 20.1 nm, 18.17 nm & 16.63 nm, respectively.

The absorption edge in UV/Vis spectra have also showed that the as-synthesized CdS, Fe-CdS, and Fe-Mn codoped CdS nanoparticles have undergone a red shifts in the absorption at approximately 400nm, 429nm and 496 nm, respectively. This can be attributed to quantum confinement effect of the CdS nanoparticles. 10 mg/L of MB dye was effectively treated (79.5 % removal) with an operating of pH 4 using 0.15 g of Fe-Mn codopedCdS nanoparticles under visible light irradiation for 2 h of irradiation time.

The reduction in absorbance of dye suggests that the dye molecules were mineralized along with color removal. It can be concluded that the Fe-Mn codopedCdS nanoparticles assisted photocatalytic degradation of textile dyes in an efficient method of waste treatment It could be as environment friendly alternative.

6. REFERENCES

Abdullah, M., Low, C. and Matthews, R.W. 1990. Effects of common inorganic anions on rates of photocatalytic oxidation of organic carbon over illuminated titanium dioxides. *Physical Chemistry,* 94: 6820-6825.

Bahnemann, M. and Haque, M.M. 2007. Titanium dioxide-mediated photocatalyzed degradation of few selected organic pollutants in aqueous suspensions. *Catalysis Today,* 124:133-148.

Baatz C., N. Decker, U. Prüße 2008 New innovative gold catalysts prepared by an improved incipient wetness method. *Journal of Catalysis* 258: 165–169

Belver, C., Bellod, R.,Stewart, S.J.,Requejo, F.G. and Fernández-García. M. 2006. Nitrogen-containing TiO_2 photocatalysts: Part 2. Photocatalytic behavior under sunlight excitation, *Applied Catalysis,* 65:309-314.

Carneiro, P. A., Osugi, M.E.,Sene, J. A., Anderson and BoldrinZanoni, M.V. 2004. Evaluation of Color removal and degradation of reactive textile azo dye on nanoporous TiO_2 thin-Film electrodes. *Electrochimica Acta,* 49:3807-3820.

Carraway, E.R., Hoffmann, A.J. and Hoffmann, M.R. 1994. Photo catalytic oxidation of organic acids on quantum-sized semiconductor colloids. *Environmental Science and Technology*, 28: 786–793.

Cohen, Z.Z., Eiden, C. and Lober, M.N. 1986. Evaluation of pesticide in ground water. *Journal of American Chemical Society,* 315: 170–196.

Cun, W., Zhao, J., Xinming, W., Bixian, M., Guoying, S. and An, P.P. 2002. Preparation, characterization and photocatalytic activity of nano-sized ZnO /SnO_2 coupled photocatalysis. *Applied Catalysis B: Environmental,* 39: 269-279.

Dabrowski, A. 2001. Adsorption from theory to practice. *Advances in colloid and interface science*, 93: 135-224.

Hullavarad, N.V., Hullavarad,S.S.and Karulkar, P.C. 2006. Review of Cadmium Sulfide CdS nanotechnology: synthesis and applications. *Journal of Nanoscience and Nanotechnology,* 8: 3272-3299.

Iorgu, A. I., Berger, D., Alexandrescu, L., Vasile, B. S. and Matei, C. 2013. Synthesis of photoluminescent pure and doped cadmium sulfide by reverse microemulsion method. *Chalcogenides Letters*, 5: 25 - 53.

Jian-xiao, L. V., Ying, C., Guo-hong, X., Ling-yun, Z. and Su-fen. W. 2011. Decoloration of methylene blue simulated wastewater using a UV-H_2O_2 combined system. *Journal of Water Reuse and Desalination,* 45:321-356.

Kato, S., Hirano, Y., Iwata, M., Sano, T., Takeuchi, K. and Matsuzawz, S. 2005. Photocatalytic degradation of gaseous sulphur compounds by silver-deposited titanium dioxide. *Journal of Applied Catalysis of Environmental Biology*. 57:109-115.

Kulkarni, J.S., Kazakova, O. and Holmes, J.D. 2006. Structural characterization on nickel doped cadmium sulfide. *Applied Physics and Material Science Process*, 85: 277-281.

Kyung, H. J., Lee, W. and Choi. 2005. Simultaneous and synergistic conversion of dyes and heavy metal ions in aqueous TiO_2 suspensions under visible-light illumination. *Environmental Science and Technol*ogy, 39: 2376–2382.

Lecheng, L. and Dacui. W. 2001. Waste water Treatment Technology of Advanced Oxidation. *Beijing:Chemical Industry Press,46:* 252-255.

Ledakowicz, S., Solecka, M. and Zylla, R. 1999. Biodegradation, decolourisation and detoxification of textile waste water enhanced by advanced oxidation processes. *Journal of Biotechnology*, 89: 175–184.

Lee, J.K., Gu, J.H. Kim, M.R. and Chun, H.S. 2001. Incineration characteristics of dye sludge in a fluidized bed incinerator. *Journal of Chemical Engineering.* 34: 171–175.

Liu,M ., Du,Y., Ma,L., Jing,D. and Guo,L. 2012. Manganese doped cadmium sulfide nanocrystal for hydrogen production from water under visible light. International *Journal of Hydrogen Energy*, 37: 730-736.

Muruganandham, M., Shobana. N. and Swaminathan, M. 2005. Optimization of solar photocatalytic degradation conditions of Reactive Yellow 14 azo dye in aqueous TiO2. *Journal of Molecular Catalysis A: Chemical*, 246: 154-161.

Ping-feng, F., Zhuo. Z., Peng, P. and Xue-gang, D. 2008. Photo degradation of methylene blue in a batch fixed bed photo reactor using activated carbon fibers supported TiO_2 photocatalyst. *The Chinese Journal of Process Engineering.* 8:1-7.

Pouretedal, H., Norozi, A., Keshavarz, M. and Semnani, A. 2009. Nanoparticles of zinc sulfide doped with manganese, nickel and copper as nanophotocatalyst in the degradation of organic dyes. *Journal of Hazardous Materiasl*, 162: 674-681.

Robinson, T., McMullan, R. and Marchant, P. 2001. Nigam and Remediation of dyes in textile effluent: a critical review on current treatment technologies with a proposed alternative. *Bioresourece Technology,* 77: 247–255.

Saien, J. and Khezrianjoo, S., 2008. Degradation of the fungicide carbendazim in aqueous solutions with UV/TiO_2 process: Optimization, kinetics and toxicity studies. *Journal of Hazardous Materials,* 157: 269-276.

Senthilkumaar, S. and Porkodi, K., 2005. Heterogeneous photocatalytic decomposition of Crystal Violet in UV-illuminated sol-gel derived nanocrystalline ZnS suspensions. *Journal of Colloid and Interface Science,* 288: 184-189.

Shifu, C., and Gengyu, C. 2005. Photocatalytic degradation of pesticides using floating photocatalyst TiO_2 and SiO_2 beads by sunlight. *Solar Energy*, 79: 1-9.

Soutsas, K., Karayannis, V., Poulios, I., Riga, A., Ntampegliotis, K., Spiliotis, X. and Papapolymerou, G.,2010. Decolorization and degradation of reactive azo dyes via heterogeneous photocatalytic processes. *Desalination*, 250: 345-350.

Sun, J., Qiao, L., Sun, S. and Wang, G., 2008. Photocatalytic degradation of methyl orange on nitrogen-doped TiO_2 catalysts under visible light and sunlight irradiation. *Journal of Hazardous Materials,* 155: 312-319.

Tang J., Zou Z., Yin J., Ye J. 2003.Photocatalytic degradation of methylene blue on $CaIn_2O_4$ under visible light irradiation. *Chemical Physics Letters*,382: 175–179.

Venkatachalam, N., Palanichamy, M., Arabindo, B. and Murugesan,V. 2007. Enhanced photocatalytic degradation of 4-chlorophenol by Zr^{4+} doped nano TiO_2. *Journal of Molecular Catalysis A,* 266: 158-165.

Verma,P., Manoj, G.S., Pandey, A.C ., 2010 . Organic capping-Effect and mechanism in Mn-doped CdS nanocomposites. *Physica B*, 405:1253–1257.

Wang, X., Yao, Z., Wang, J., Guo, W. and Li, G. 2008. Degradation of reactive brilliant red in aqueous solution by ultrasonic cavitation. *Ultrasonics Sonochemistry*, 15: 43-48.

Winsor, P. 1948. Hydrotropy, solubilization, and related emulsification processes. *Journal of Chemical Society Faraday Trans*, 44: 376-382.

Wu, T., Liu, G. Zhao, J., Hidaka, H. and Serpone, N. 1999. Evidence for H_2O_2 generation during the TiO_2-assisted photodegradation of dyes in aqueous dispersions under visible light illumination. *Physcal Chemistry,* 103 (23): 4862-4867.

Zainal, Z., Hui, L.H., Hussein, M.Z. and Ramli, I. 2005. Removal of dyes using immobilized tita nium dioxide illuminated by fluorescent lamps. *Journal of Hazardous Materials*,125:113-12.

Zhan, H. Q., H. Tian. 1998. Photo Catalytic Degradation of Acid Azo Dyes in Aqueous TiO_2 Suspension the Effect of Substituent's. *Dyes and Pigments*,37: 231-239.

Zhao, J., Chen, C. and Ma, W.2005.Photocatalytic degradation of organic pollutants under visible light irradiation. *Russian Journal of Inorganic Chemistry,* 35: 269-278.

Zhu, X., Yuan, C., Bao, Y., Yang, J. and Wu, Y. 2005. Photocatalytic degradation of pesticide pyridaben on TiO_2 particles. *Journal of Molecular Catalysis*, 229:95-105.

7. APPENDIX

Appendix table 1. Point of zero charge determination of Fe,Mn:co-doped CdS photocatalyst.

pH	pH values												
pHi	1.01	1.95	2.99	4.01	4.98	6.01	6.88	8.01	8.96	10.21	11.13	12.03	13.11	13.98
pHf	1.13	2.1	3.04	4.04	5.01	6.03	6.76	7.9	8.86	10.16	11.06	11.94	13.03	13.89
ΔpH	0.12	0.15	0.05	0.03	0.03	0.02	-0.12	-0.11	-0.1	-0.05	-0.07	-0.09	-0.08	-0.09

Appendix Table 2. Percentage degradation of MB as a function of time under visible radiation using different as-synthesized photocatalysts.

Time(min)	NO Cat. %Degr.	CdS %Degr.	FC %Degr.	MC %Degr.	FMC %Degr.
0	0	0	0	0	0
20	0.1	21.5	22.8	23.2	35.4
40	0.4	42.6	39.7	40.3	45.1
60	0.6	49.1	41.3	42.5	55.7
80	0.7	55.0	53.3	54.4	64.2
100	0.9	60.3	62.6	64.4	75.4
120	1.1	69.4	72.6	75.6	79.5

Appendix Table 3. Plot of percent degradation of MB as function of time by varying the pH of the solution keeping both MB dye and photocatalyst amounts constant.

Time(min)	2	4	6	8	10	11
0	0	0	0	0	0	0
20	2.5	14.9	6.8	8.2	6.3	1.8
40	6.3	23.1	14.9	14.8	10.7	4.9
60	12.0	35.9	28.4	20.1	19.4	10.2
80	15.1	40.0	36.2	30.5	28.9	12.4
100	27.8	53.9	40.5	34.8	33.4	18.7
120	35.2	61.9	43.0	39.1	37.0	22.4

Appendix table 4. Photocatalytic degradation efficiency of MB as a function of time by varying the amount of Fe,Mn:CdS photocatalyst and keeping amount of MB dye constant.

Time (min)	%Degr. 50mg/L	%Degr. 100mg/L	%Degr. 150mg/L	%Degr. 200mg/L	%Degr. 250mg/L
0	0	0	0	0	0
20	5.9	13.1	14.3	12.8	7.4
40	9.8	19.9	21.7	17.9	10.1
60	14.5	23.3	29.2	25.6	17.2
80	19.6	29.1	49.6	30.1	23.8

100	27.2	35.4	62.1	36.5	31.3
120	31.8	38.3	69.6	44.8	33.9

Appendix Table 5.Photocatalytic degradation efficiency MB dye as a function of time by varying the amount of dye solution and keeping constant photocatalyst amount.

Time (min)	%Degr. 10mg/L	%Degr. 20mg/L	%Degr. 30mg/L	%Degr. 40mg/L	%Degr. 50mg/L
0	0	0	0	0	0
20	3.5	4.9	4.7	3.6	2.3
40	8.9	5.9	6.6	5.3	4.4
60	13.4	8.3	8.1	7.3	7.2
80	22.4	16.5	12.9	10.5	11.6
100	25.3	22.3	19.9	14.3	12.9
120	30.3	24.4	21.8	18.7	17.5

Fe,Mn:CdS = 150 mg/L, λ_{max} = 661 nm, pH = 4

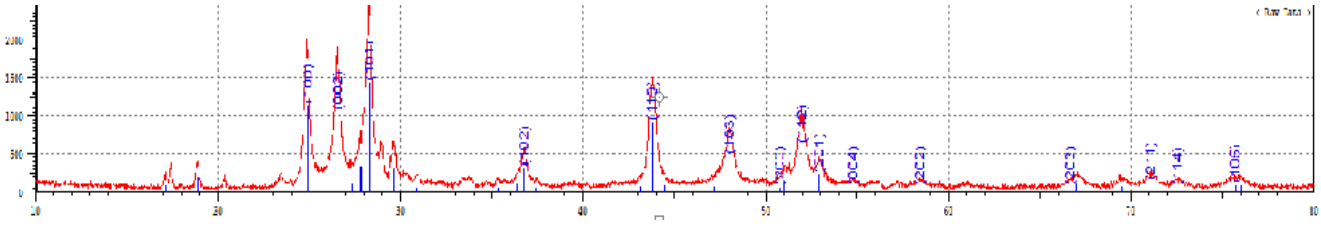

Appendix Figure 1.XRD pattern of CdS nanoparticles

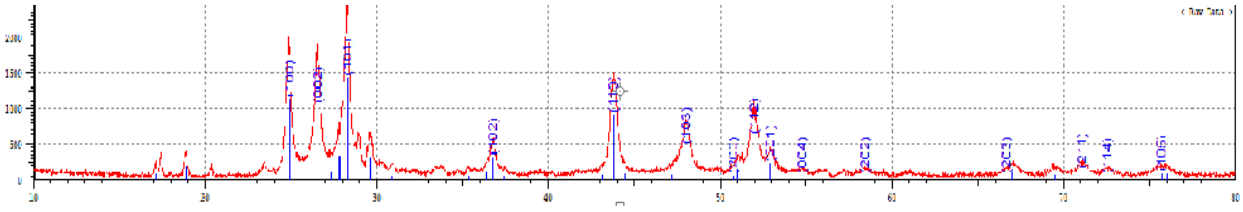

Appendix Figure 2.XRD pattern of Fe:CdS nanoparticles

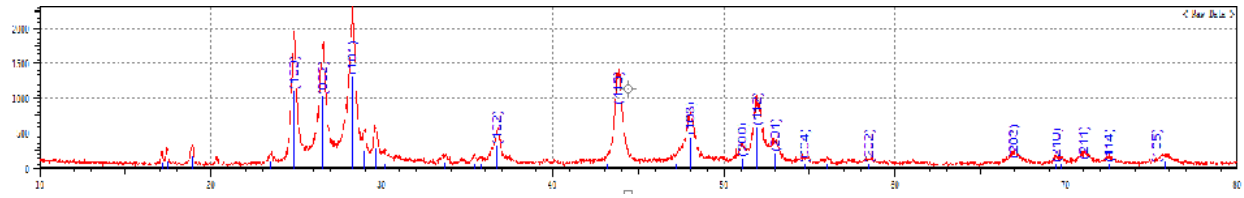

Appendix Figure 3.XRD pattern of Mn:CdS nanoparticles

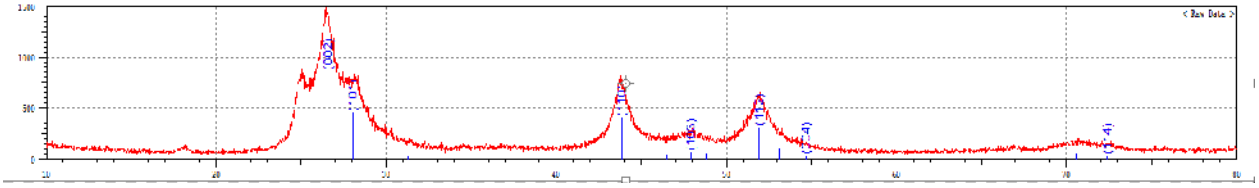

Appendix Figure 4.XRD pattern of Fe,Mn:CdS nanoparticles